ELSEVIER

2 October 1997

PHYSICS LETTERS B

Physics Letters B 410 (1997) 344–352

Study of $\bar{n}p$ annihilation in two mesons in the momentum range between 50 to 400 MeV/c with OBELIX

OBELIX Collaboration

A. Bertin [a], M. Bruschi [a], M. Capponi [a], A. Collamati [a], S. De Castro [a], R. Donà [a], A. Ferretti [a], L. Filippi [a], D. Galli [a], B. Giacobbe [a], U. Marconi [a], I. Massa [a], M. Piccinini [a], M. Poli [a,1], N. Semprini-Cesari [a], R. Spighi [a], V. Vagnoni [a], S. Vecchi [a], A. Vezzani [a], F. Vigotti [a], M. Villa [a], A. Vitale [a], A. Zoccoli [a], M. Corradini [b], A. Donzella [b], E. Lodi Rizzini [b], L. Venturelli [b], A. Zenoni [b], C. Cicaló [c], A. Masoni [c], G. Puddu [c], S. Serci [c], P. Temnikov [c,2], G. Usai [c], O. E.Gorchakov [d], S.N. Prakhov [d], A. M.Rozhdestvensky [d], M.G. Sapozhnikov [d], V.I. Tretyak [d], P. Gianotti [e], C. Guaraldo [e], A. Lanaro [e], V. Lucherini [e], F. Nichitiu [e,3], C. Petrascu [e,3], A. Rosca [e,3], V. G.Ableev [f,4], C. Cavion [f], U. Gastaldi [f], M. Lombardi [f], G. Maron [f], L. Vannucci [f], G. Vedovato [f], G. Bendiscioli [g], V. Filippini [g], A. Fontana [g], P. Montagna [g], A. Rotondi [g], A. Saino [g], P. Salvini [g], C. Scoglio [g], M. Agnello [i], F. Balestra [h], E. Botta [h], T. Bressani [h], M.P. Bussa [h], L. Busso [h], D. Calvo [h], P. Cerello [h], S. Costa [h], O. Denisov [h,4], L. Fava [h], A. Feliciello [h], L. Ferrero [h], A. Filippi [h], R. Garfagnini [h], A. Grasso [h], F. Iazzi [i], A. Maggiora [h], S. Marcello [h], B. Minetti [i], D. Panzieri [h], D. Parena [h], E. Rossetto [h], F. Tosello [h], L. Valacca [h], G. Pauli [j], S. Tessaro [j], L. Santi [k], A.E. Kudryavtsev [l]

[a] *Dipartimento di Fisica, Univ. di Bologna and INFN, Sez. di Bologna, Bologna, Italy*
[b] *Dipartimento di Chimica e Fisica per l'Ingegneria e per i Materiali, Univ. di Brescia and INFN, Sez. di Pavia, Pavia, Italy*
[c] *Dipartimento di Fisica, Univ. di Cagliari and INFN, Sez. di Cagliari, Cagliari, Italy*

[1] Dipartimento di Energetica "Sergio Stecco", Univ. di Firenze, Firenze, Italy.
[2] On leave of absence from Institute for Nuclear Research and Nuclear Energy, Sofia, Bulgaria.
[3] On leave of absence from National Institute of Research and Devolopment for Physics and Nuclear Engineering "Horia Hulubei", Bucharest-Magurele, Romania.
[4] On leave of absence from Joint Institute for Nuclear Research, Dubna, Moscow, Russia.

PII S0370-2693(97)00938-6

[d] Joint Institute of Nuclear Research, Dubna, Moscow, Russia
[e] Laboratori Nazionali di Frascati dell'INFN, Frascati, Italy
[f] Laboratori Nazionali di Legnaro dell'INFN, Legnaro, Italy
[g] Dipartimento di Fisica Nucleare e Teorica, Univ. di Pavia and INFN Sez. di Pavia, Pavia, Italy
[h] Istituto di Fisica, Univ. di Torino and INFN, Sez. di Torino, Torino, Italy
[i] Politecnico di Torino and INFN, Sez. di Torino, Torino, Italy
[j] Istituto di Fisica, Univ. di Trieste and INFN, Sez. di Trieste, Trieste, Italy
[k] Istituto di Fisica, Univ. di Udine and INFN, Sez. di Trieste, Trieste, Italy
[l] Theory Division ITEP, Moscow, Russia

Received 7 May 1997; revised 19 June 1997
Editor: L. Montanet

Abstract

We measured the in flight annihilation frequencies and cross sections of reactions $\bar{n}p \to \pi^+\pi^0, \pi^+\eta$ and K^+K_S in the antineutron momentum range between 50 and 400 MeV/c. The annihilation frequencies of these channels from the different allowed initial states were calculated and some information about the $\bar{n}p$ annihilation dynamics were obtained. The first determination of the D-wave contribution in this momentum range was also obtained. © 1997 Published by Elsevier Science B.V.

PACS: 13.75.Cs; 14.40.Aq

Keywords: Nucleon-nucleon interactions (including antinucleons, deuterons, etc.); π, K and η mesons

1. Introduction

Among the low energy $\bar{N}N$ experiments OBELIX can study either the $\bar{p}p$ or the pure $I = 1$ $\bar{n}p$ interaction by means of a unique facility for the production of antineutrons ($\bar{n}$). This has the advantage, with respect to the $\bar{p}n$ annihilation in deuterium, of the absence of the rescattering problem due to the spectator proton. Moreover, while a systematic study of $\bar{p}p$ annihilation is already available, few data on $\bar{n}p$ total cross sections and no data on annihilation frequencies and cross sections of specific $\bar{n}p$ reactions at low energy are available. In this letter we present the first exclusive measurement of annihilation frequencies of the channels:

$$\bar{n}p \to \pi^+\pi^0 \quad (1)$$

$$\bar{n}p \to \pi^+\eta \quad (2)$$

$$\bar{n}p \to K^+K_S \quad (3)$$

in the $\bar{n}$ momentum range between 50 and 400 MeV/c, with the aim of investigating:

i) the dynamic of annihilation from the pure $I = 1$ state;

ii) the contribution of the different partial waves to the $\bar{N}N$ $I = 1$ annihilation.

To this goal we define the annihilation frequency of a channel ch as:

$$f_{ch}(p_{\bar{n}}) = \frac{N_{ch}(p_{\bar{n}})}{\epsilon_{ch}(p_{\bar{n}})} \cdot \frac{1}{N^{ANN}(p_{\bar{n}})} \quad (4)$$

where $N_{ch}(p_{\bar{n}})$ and $\epsilon_{ch}(p_{\bar{n}})$ are respectively the number of selected events and the reconstruction efficiency of channel ch, and $N^{ANN}(p_{\bar{n}})$ is the total number of annihilations in the reaction target as a function of $\bar{n}$ momentum ($p_{\bar{n}}$). In order to study the dependence of the annihilation frequencies on the initial energy, the $\bar{n}$ momentum spectrum was divided in three intervals: 50–150, 150–250 and 250–400 MeV/c.

The two-body channels are the most suitable reactions to study both the dynamical effects of the $\bar{N}N$ annihilation process and the dependence of the annihilation frequencies on the initial state. In fact the selection rules imposed by quantum numbers conservation restrict the number of the allowed initial states giving the possibility to study their contributions separately. For example, assuming only S, P and D waves contributions to the annihilation in flight below 400 MeV/c [1,2], reactions (1)–(3) can be produced only from the states shown in Table 1. The

Table 1
Selection rules for the initial states of reactions (1)–(3). P = parity forbidden state; G = G-parity forbidden state; * = allowed state

$\bar{n}p$	$^1S_0$	$^3S_1$	$^1P_1$	$^3P_0$	$^3P_1$	$^3P_2$	$^1D_2$	$^3D_1$	$^3D_2$	$^3D_3$
$\pi^+\pi^0$	P	*	P	G	P	G	P	*	P	*
$\pi^+\eta$	P	G	P	*	P	*	P	G	P	G
K^+K_S	P	*	P	*	P	*	P	*	P	*

production of channels (1)–(3) from the different allowed initial states will be studied in Section 3.

In this letter we also report on the contribution of D wave to the annihilation up to 400 MeV/c using the measurement of the annihilation frequencies of reactions (1)–(3) as a function of the $\bar{n}$ momentum.

2. Measurement of annihilation frequencies

A detailed description of the OBELIX apparatus is given elsewhere [3]. For the present measurement the Jet Drift Chamber (JDC), the time of flight system (TOF) and the high angular resolution gamma detector (HARGD) were used together with the $\bar{n}$ beam line [4–6]. The antineutron momentum is measured event by event by a time of flight measurement as described in [4–6]. About $1.3 \cdot 10^7$ events were collected with a *minimum bias trigger* defined as the *OR* of the internal TOF barrel giving a signal within a 120 ns time gate opened by the $\bar{n}$ beam counting system. The events include annihilations in the 25 cm long 7 cm radius liquid hydrogen reaction target and in nuclear targets placed behind it in order to measure the $\bar{n}$ annihilation cross section on different nuclei (these events were not considered in this analysis).

To select reactions (1) and (2) the following general cuts were applied: i) one track with positive charge and length $L > 40$ cm in the JDC for a good momentum reconstruction; ii) maximum approaching point of the track to the beam axis (assumed as interaction vertex) within a fiducial volume in the reaction target ($|z| < 12$ cm, $R < 7$ cm); iii) two neutral clusters in the gamma detector. A two constraint (2C) kinematic fit was then used to test the hypothesis $\bar{n}p \to \pi^+\gamma\gamma$. We applied different cuts on the measured π^+ momentum ($|p_{\pi^+}|$), χ^2 probability (P_{χ^2}) and π^0 center of mass decay angle cosine ($Q_{\gamma\gamma}$) to test the result stability. The $\gamma\gamma$ invariant mass distribution with $P_{\chi^2} > 0.15$ and $|p_{\pi^+}| > 0.65$ GeV/c is shown in Fig. 1a in which the

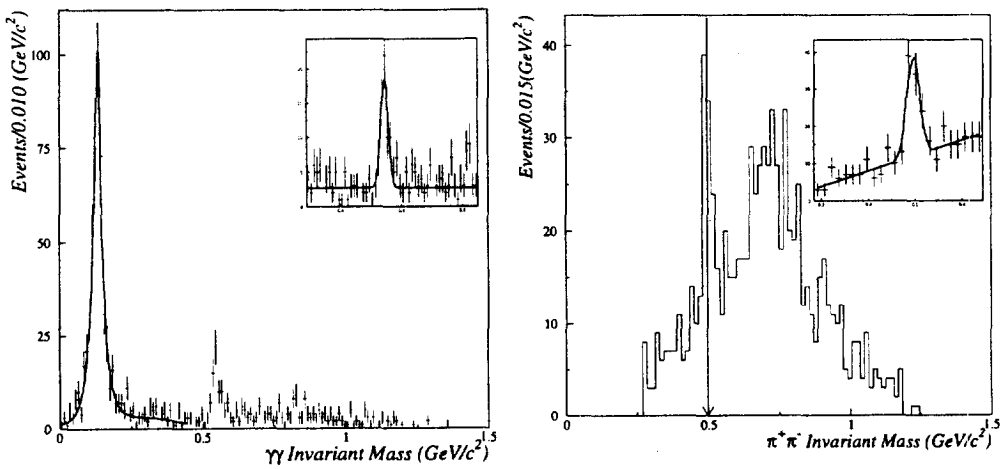

Fig. 1. (a) $\gamma\gamma$ invariant mass distribution for events selected with a 2C kinematic fit. In the inset the fit in the η region is shown. (b) $\pi^+\pi^-$ invariant mass distribution for events selected with a 4C kinematic fit. In the inset the fit in the K_S region is shown.

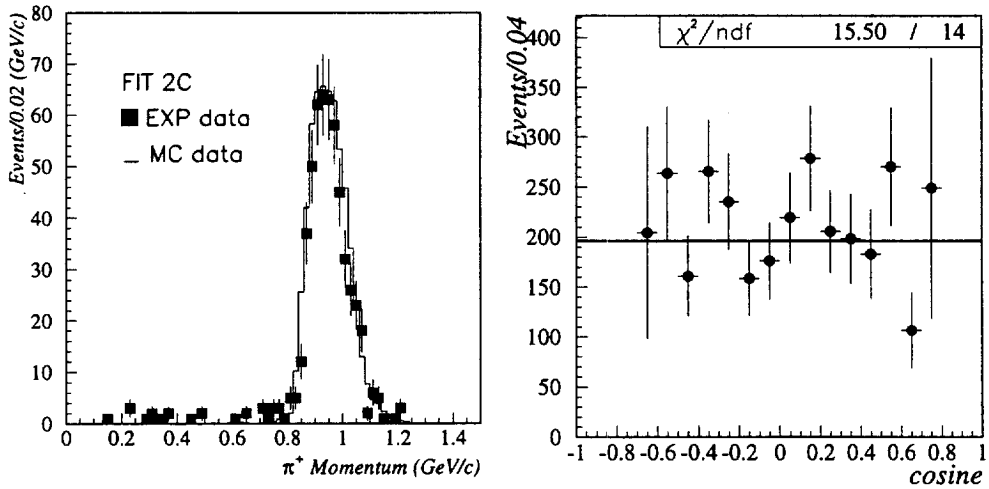

Fig. 2. (a) π^+ momentum distribution for $\pi^+\pi^0$ events selected with a 2C kinematic fit. (b) Center of mass cosine of the angle between the π^+ direction and the beam axis.

signals of π^0 and η can be clearly observed with a background contribution of about 15% and 30% respectively. The π^0 peak was fitted with the distribution of Ref. [7] plus a polynomial background, while the η peak by a gaussian distribution plus a flat background. The obtained masses and experimental widths are: $M_{\pi^0} = 134 \pm 1\,\mathrm{MeV/c^2}$ with $\sigma_{\pi^0} \sim 18\,\mathrm{MeV/c^2}$ and $M_\eta = 546 \pm 4\,\mathrm{MeV/c^2}$ with $\sigma_\eta \sim 14\,\mathrm{MeV/c^2}$.

To select reaction (3) we required: i) three tracks with total charge +1 in the JDC and length $L > 40$ cm; ii) reconstructed vertex, which is necessarily the K_S decay vertex, within the fiducial volume. This was necessary to avoid the background due to $\bar{n}$ annihilations outside the reaction target. As the mean K_S mean path before decay is about 4 cm, most of K_S decay inside the fiducial volume. A four constraint (4C) kinematic fit was then used to test the hypothesis $\bar{n}p \to K^+\pi^+\pi^-$. Also in this case we applied different cuts on the $|p_{K^+}|$ and P_{χ^2} distributions obtaining results compatible among each other. In Fig. 1b the $\pi^+\pi^-$ invariant mass distribution with $|p_{K^+}| > 0.6\,\mathrm{GeV/c}$ and $P_{\chi^2} > 0.05$ is shown from which the K_S signal can be clearly observed

Table 2
Reconstruction efficiency ϵ_{ch} and number of counted events of reactions (1)–(3) after background subtraction

Reaction	$p_{\bar{n}}$ (MeV/c)	$N_{ch} \pm \delta N_{ch}$	$\epsilon_{ch} \pm \delta\epsilon_{ch}$
$\pi^+\pi^0$	50–150	31 ± 6	0.112 ± 0.007
	150–250	83 ± 14	0.115 ± 0.004
	250–400	163 ± 16	0.109 ± 0.002
$\pi^+\eta$	50–150	< 7 *	0.042 ± 0.004
	150–250	13 ± 4	0.046 ± 0.003
	250–400	47 ± 9	0.041 ± 0.002
$K^+K^0_S$	50–150	8 ± 3	0.076 ± 0.006
	150–250	12 ± 4	0.075 ± 0.003
	250–400	47 ± 13	0.071 ± 0.002

* 90% confidence level

Table 3
Efficiency for detection of annihilations and total number of annihilations in the three selected momentum intervals

$p_{\bar{n}}$(MeV/c)	$\epsilon^{ANN} \pm \delta\epsilon^{ANN}_{st} \pm \delta\epsilon^{ANN}_{syst}$	$N^{ANN} \pm \delta N^{ANN}_{st} \pm \delta N^{ANN}_{syst}$
50–150	$0.49 \pm 0.03_{st} \pm 0.05_{syst}$	$(1.66 \pm 0.10_{st} \pm 0.17_{syst}) \cdot 10^5$
150–250	$0.48 \pm 0.02_{st} \pm 0.04_{syst}$	$(5.70 \pm 0.24_{st} \pm 0.46_{syst}) \cdot 10^5$
250–400	$0.48 \pm 0.02_{st} \pm 0.04_{syst}$	$(16.56 \pm 0.69_{st} \pm 1.40_{syst}) \cdot 10^5$

over a background mainly due to $K^+K^-\pi^+$ and $\pi^+\pi^+\pi^-$. The fit of K_S peak with a gaussian distribution plus a first order polynomial background gives $M_{K_S} = 499 \pm 3\ \mathrm{MeV/c^2}$ and $\sigma_{K_S} \sim 14\ \mathrm{MeV/c^2}$.

The number of selected events in the three momentum intervals for reactions (1)–(3) is shown in Table 2.

In order to calculate the selection efficiency ϵ_{ch} for the three reactions about 50000 events were simulated for each channel using the OBELIX Monte Carlo code based on the GEANT package [8], which provides the simulation of geometry, efficiencies and resolutions of the detectors and timing gates for the trigger. In Fig. 2a the measured π^+ momentum spectrum is shown for Monte Carlo $\pi^+\pi^0$ events and experimental data selected by the 2C fit within 3σ around the π^0 mass. A good agreement can be observed. For the $\pi^+\pi^0$ and $\pi^+\eta$ channels, the angular distributions were simulated according to the allowed initial states. In Fig. 2b, for example, the center of mass cosine of the angle between the π^+ direction and the beam axis is shown for the experimental data and it is compatible with the expected flat S-wave distribution. For the K^+K_S channel the results obtained with S and P wave angular distributions turn out to be compatible; we then used for simplicity the S wave angular distribution.

In Table 2 the efficiencies for reactions (1)–(3) are also reported for the three momentum intervals.

To obtain the normalization to the annihilating beam we counted the number of recorded events (N_{count}) satisfying the following criteria: i) number of tracks in the JDC greater than 2 in order to have a good vertex reconstruction; ii) annihilation vertex within the reaction target. The efficiency for the detection of the annihilations with a correct measurement of the $\bar{n}$ momentum was determined by means of Monte Carlo simulations. All channels with total pion multiplicity up to 6 were simulated ($\pi^+ m\pi^0$,$0 < m < 6$; $2\pi^+\pi^- m\pi^0$,$m < 4$; $3\pi^+ 2\pi^- m\pi^0$,$m < 2$) as well as some kaonic channels (K^+K_S, $K^+K_S\pi^0$) with statistics from 50000 to 150000 events each, and submitted to criteria i)-ii). The total efficiency was then obtained by weighting the efficiencies (ϵ_j) for the different channels (j) with the charge conjugated $\bar{p}n$ branching ratios ($BR_j(LD_2)$) measured in liquid deuterium [9–12]:

$$\epsilon^{ANN} = \sum_j \epsilon_j \cdot BR_j(LD_2) \cdot \frac{1}{\sum_j BR_j(LD_2)} \qquad (5)$$

where the sum is running over the simulated channels. The assumption made by using the normalization factor is that reactions with unknown $BR_j(LD_2)$

Table 4
Annihilation frequencies for reactions (1)–(3) in the three selected momentum intervals

Ch	$f(10^{-3})$		
	[50–150] MeV/c	[150–250] MeV/c	[250–400] MeV/c
$\pi^+\pi^0$	$1.67 \pm 0.35_{st} \pm 0.17_{sys}$	$1.26 \pm 0.22_{st} \pm 0.10_{sys}$	$0.90 \pm 0.10_{st} \pm 0.08_{sys}$
$\pi^+\eta$	< 0.97 *	$0.49 \pm 0.15_{st} \pm 0.04_{sys}$	$0.69 \pm 0.14_{st} \pm 0.06_{sys}$
$K^+K^0_S$	$0.92 \pm 0.37_{st} \pm 0.09_{sys}$	$0.41 \pm 0.14_{st} \pm 0.03_{sys}$	$0.58 \pm 0.16_{st} \pm 0.05_{sys}$

* 90% confidence level.

Table 5
Total $\bar{n}p$ annihilation cross section and annihilation cross sections for reactions (1)–(3) in the three momentum intervals integrated in the angular range. Statistical and systematic errors were summed quadratically

Ch	σ_{ann} (mb)		
	[50–150] MeV/c	[150–250] MeV/c	[250–400] MeV/c
Total (this work)	222 ± 29	192 ± 23	141 ± 17
Total [14]	250 ± 40	186 ± 15	140 ± 12
$\pi^+\pi^0$	0.370 ± 0.080	0.244 ± 0.053	0.128 ± 0.018
$\pi^+\eta$	< 0.2 *	0.096 ± 0.031	0.098 ± 0.021
$K^+K^0_S$	0.205 ± 0.080	0.079 ± 0.027	0.082 ± 0.024

* 90% confidence level.

have, in average, the same detection efficiency as the known ones. As the sum of known $BR_j(LD_2)$ is close to one, this assumption is acceptable. The total number of annihilations in the target in each momentum interval is then obtained as:

$$N^{\mathrm{ANN}} = \frac{N_{\mathrm{count}}}{\epsilon^{\mathrm{ANN}}} \tag{6}$$

In the determination of statistical errors on N^{ANN}, uncertainties on the $BR_j(LD_2)$ dominate over statistical errors of the generated channels. For the determination of systematic errors the following procedure was adopted: an upper limit for efficiency was determined assuming the branching ratio of all reactions with a given charged multiplicity (for example $2\pi^+\pi^- m\pi^0$) as branching ratio of the reaction, with that multiplicity, showing the highest efficiency ($2\pi^+\pi^-$). In a similar way a lower limit for efficiency was determined. The maximum difference between ϵ^{ANN} and these limits was taken as systematic error. This takes into account both uncertainties in the knowledge of some $BR_j(LD_2)$ and the fact that no dynamics was simulated. It has to be noted that, due to the dominance of channels with high multiplicity in the counting procedure of annihilations given by criterion ii), the effects of dynamics are averaged. The interference between the different $\bar{n}$ momentum intervals was also evaluated and turned out to be negligible. The reconstruction efficiency and the total number of annihilations are reported in Table 3.

The measured annihilation frequencies, calculated from Eq. (4), are reported in Table 4 for the three momentum intervals.

We also determined the annihilation cross sections of reactions (1)–(3) in the three momentum intervals as:

$$\sigma_{\mathrm{ch}}(i) = \frac{1}{\rho \cdot N_{\mathrm{Av}} \cdot \Delta z} \cdot \frac{N_{\mathrm{ch}}(i)}{\epsilon_{\mathrm{ch}}(i)} \cdot \frac{1}{N_{\bar{n}}(i)}, \quad i = 1,3 \tag{7}$$

were ρ is the liquid hydrogen density (0.0708 g/cm^3), N_{Av} is the Avogadro number, Δz is the fiducial volume length and $N_{\bar{n}}$ is the number of incident antineutrons. The number of antineutrons was obtained from the total number of antiprotons entering the production target as counted by the OBELIX counting system, and from the evaluation of the flux of the $\bar{n}$ beam. For the geometry of the date relevant to this analysis the beam was $36 \pm 1\,\bar{n}/10^6\bar{p}$.

Using this value and the total number of annihilations N^{ANN} in the reaction target (see Table 3) we obtained for the total annihilation $\bar{n}p$ cross section in the three momentum intervals the values reported in Table 5 where the errors are dominated by systematics due to the annihilation counting procedure and to the fluctuations of the spot of the $\bar{p}$ beam [13]. These values are in very good agreement with the values obtained by integrating in the three momentum intervals previous OBELIX measurements [14] performed in a different geometrical setup (also reported in Table 5). A direct comparison can be done also with a previous measurement [15] in the momentum intervals between 150 and 250 MeV/c and between 250 and 400 MeV/c giving respectively 189 ± 90 mb and 132 ± 60 mb. The agreement among the results is very good.

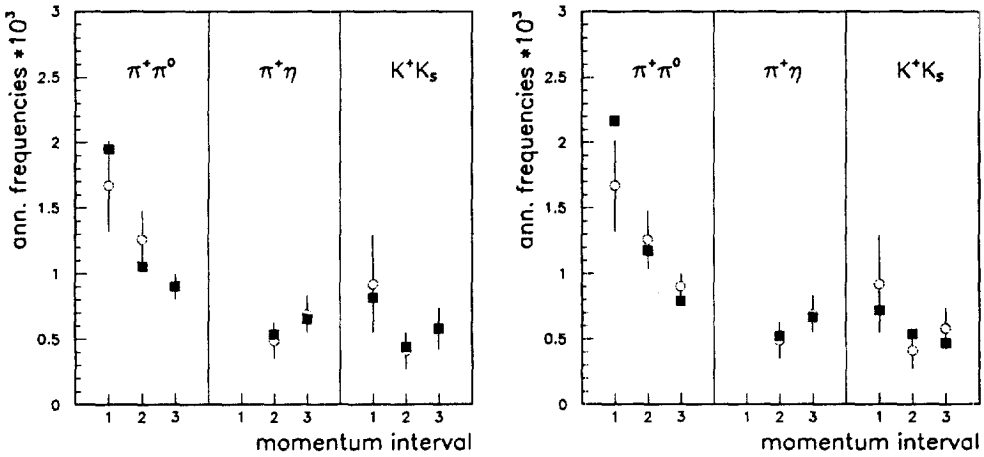

Fig. 3. Measured annihilation frequencies (circles) and values obtained from the fit of system (17) (squares) with the assumptions of CC model for S wave percentage as a function of the $\bar{n}$ momentum interval (see text). a) α_D free; b) α_D set to zero.

The annihilation cross sections of reactions (1)–(3), obtained from Eq. (7) and using the values of Table 2 in the three momentum intervals, are also reported in Table 5.

3. Discussion of the results

We can define the annihilation frequency of a channel *ch* in the *i-th* momentum interval as [16]:

$$f_{\rm ch}(i) = \sum_L \alpha_L(i) W_{\rm ch}^L \tag{8}$$

where the sum is running over the possible initial partial waves of angular momentum L, $\alpha_L(i)$ are the corresponding annihilation fractions and $W_{\rm ch}^L$ are the branching ratios of channel *ch* from the initial states of angular momentum L.

Using this approach, we made the following assumptions in our analysis:

i) only S and P waves contribute to annihilation up to about 250 MeV/c [2] ($\alpha_P(i) = 1 - \alpha_S(i), i = 1,2$);

ii) S, P and D wave contribute to annihilation between 250 and 400 MeV/c [1] ($\alpha_P(3) = 1 - \alpha_S(3) - \alpha_D(3)$);

iii) $W_{\rm ch}^L$ are independent of the $\bar{n}$ momentum in the range of interest;

iv) the S-wave fraction

$$\alpha_S = \frac{\sigma_{\rm ann}^S}{\sigma_{\rm ann}^S + \sigma_{\rm ann}^P} \tag{9}$$

is calculated from: 1) the Dover-Richard (DR) potential model [1] and 2) the coupled-channel model (CC) of Ref. [17].

Using Eq. (8) for reactions (1)–(3) in the three momentum intervals, we can write the following system:

$$\begin{aligned}
f_{\pi^+\pi^0}(1) &= h\alpha_S(1) W_{\pi^+\pi^0}^0 \\
f_{\pi^+\pi^0}(2) &= \alpha_S(2) W_{\pi^+\pi^0}^0 \\
f_{\pi^+\pi^0}(3) &= \alpha_S(3) W_{\pi^+\pi^0}^0 + \alpha_D(3) W_{\pi^+\pi^0}^2 \\
f_{\pi^+\eta}(2) &= (1 - \alpha_S(2)) W_{\pi^+\eta}^1 \\
f_{\pi^+\eta}(3) &= (1 - \alpha_S(3) - \alpha_D(3)) W_{\pi^+\eta}^1 \\
f_{K^+K_S}(1) &= \alpha_S(1) W_{K^+K_S}^0 + (1 - \alpha_S(1)) W_{K^+K_S}^1 \\
f_{K^+K_S}(2) &= \alpha_S(2) W_{K^+K_S}^0 + (1 - \alpha_S(2)) W_{K^+K_S}^1 \\
f_{K^+K_S}(3) &= \alpha_S(3) W_{K^+K_S}^0 + (1 - \alpha_S(3) - \alpha_D(3)) \\
&\quad \times W_{K^+K_S}^1 + \alpha_D(3) W_{K^+K_S}^2
\end{aligned} \tag{10}$$

of 8 equations and 7 parameters ($W_{\rm ch}^L$ terms and $\alpha_D(3)$). The fit of this system with respect to these parameters gives the values shown in Table 6 for the two models.

In Fig. 3a the measured annihilation frequencies and those obtained from the fit of system (17) are shown using the coupled channel model's predictions for α_S. To check the sensibility of the fit to α_D, this parameter was also set to zero (Fig. 3b). A

Table 6
Values of the branching ratios of reactions (1)–(3) and $\alpha_D(3)$ obtained from the fit with CC (χ^2/ndf = 1.9/1) and DR (χ^2/ndf = 1.4/1) hypotheses

	$W^0_{\pi^+\pi^0}$ (10^{-3})	$W^2_{\pi^+\pi^0}$ (10^{-3})	$W^1_{\pi^+\eta}$ (10^{-3})	$W^0_{K^+K_S}$ (10^{-3})	$W^1_{K^+K_S}$ (10^{-3})	$W^2_{K^+K_S}$ (10^{-3})	α_D %
CC	2.3 ± 0.4	6.1 ± 2.2	0.99 ± 0.22	0.95 ± 0.16	0.01 ± 0.19	9.7 ± 3.3	3.0 ± 1.5
DR	2.3 ± 0.4	5.9 ± 1.6	0.99 ± 0.22	0.92 ± 0.23	0.01 ± 0.23	7.2 ± 5.9	4.6 ± 2.8

worsening of the normalized χ^2 from 1.9 (CL $\sim$ 20%) to 3.4 (CL $\sim$ 6%) was found, suggesting the presence of a non negligible D-wave contribution.

The results of Table 5 were elaborated as follows:

1. From the measurement of $W^0_{\pi^+\pi^0}$ and $W^0_{K^+K_S}$, the elementary branching ratios of reactions (1) and (3) from $^{33}S_1$ state can be calculated. We can define the elementary branching ratios $W_{ch}(J^P)$ of a channel *ch* from the states J^P with angular momentum L as [16]:

$$W^L_{ch} = \sum_{J^P \in L} \frac{\alpha(J^P)}{\alpha_L} W_{ch}(J^P) \tag{11}$$

Assuming statistical population of the initial states we can write:

$$\sigma^S_{ann} = \sigma_{ann}\left(^3S_1\right) + \sigma_{ann}\left(^1S_0\right) = \tfrac{3}{4}\sigma^S_{ann} + \tfrac{1}{4}\sigma^S_{ann}$$

$$\Rightarrow \alpha\left(^3S_1\right) = \frac{\sigma_{ann}\left(^3S_1\right)}{\sigma^S_{ann} + \sigma^P_{ann}} = \tfrac{3}{4}\alpha_S. \tag{12}$$

For reactions (1) and (3) it thus turns out that:

$$W_{\pi^+\pi^0}\left(^3S_1\right) = \tfrac{4}{3}W^0_{\pi^+\pi^0} = (3.1 \pm 0.5) \cdot 10^{-3} \tag{13}$$

$$W_{K^+K_S}\left(^3S_1\right) = \tfrac{4}{3}W^0_{K^+K_S} = (1.3 \pm 0.2) \cdot 10^{-3}. \tag{14}$$

2. Using the K^+K_S elementary branching ratio from $^{33}S_1$ state and the K^+K^- and $K^0\overline{K}^0$ elementary branching ratios from $^3S_1$ state ($I = 0,1$), it is possible to separate the contributions to the $K\overline{K}$ production amplitude from the singlet and triplet isospin states. If M_0 and M_1 are the $I = 0$ and $I = 1$ $K\overline{K}$ production amplitudes one can write [18], neglecting the $\bar{p}p - \bar{n}n$ interference:

$$|M_0|^2 = BR_{K^+K^-}\left(^3S_1\right) + BR_{K^0\overline{K}^0}\left(^3S_1\right) - |M_1|^2. \tag{15}$$

Using the $BR_{K^+K^-}(^3S_1)$ and $BR_{K^0\overline{K}^0}(^3S_1)$ values measured in $\bar{p}p$ annihilation at rest [16]:

$$BR_{K^+K^-}\left(^3S_1\right) = (1.44 \pm 0.08) \cdot 10^{-3},$$

$$BR_{K^0\overline{K}^0}\left(^3S_1\right) = BR_{K_SK_L} = (1.36 \pm 0.09) \cdot 10^{-3} \tag{16}$$

and $W_{K^+K_S}(^3S_1)$ from the present analysis [5]

$$|M_1|^2 = \tfrac{1}{2}W_{K^+\overline{K}^0}\left(^3S_1\right) = W_{K^+K_S}\left(^3S_1\right)$$

$$= (1.3 \pm 0.2) \cdot 10^{-3} \tag{17}$$

one obtains, from Eq. (22):

$$\frac{|M_1|^2}{|M_0|^2} = 0.9 \pm 0.2 \tag{18}$$

which shows that the $K\overline{K}$ amplitudes from $I = 0$ and $I = 1$ S-wave initial states are comparable. This result cannot be compared with the one stated in [1,18] and [19] where a wrong formula was used (see footnote).

3. The value of $W^1_{K^+K_S}$ obtained from the fit of system (17) is compatible with zero suggesting a suppression of the channel $K^+\overline{K}^0$ from P-wave. A similar behaviour was found in other two-body channels both in $\bar{p}p$ and $\bar{n}p$ annihilation. For example the $\bar{p}p \to K^+K^-$ branching ratio ($I = 0,1$) decreases by a factor of about 4 going from S-wave to P-wave, while the $\bar{p}p \to \phi\pi^0$ and $\bar{n}p \to \phi\pi^+$ reactions, which come from pure $I = 1$ state, have production rates from P-wave compatible with zero [20,21]. Moreover a general suppression rule for $(0^{-+},1^{--})$ two-body final states from $^1P_1$ $I = 1$ initial state has

[5] In the similar formula (35) used in Ref. [18] a factor 1/2 is missing.

been recently suggested [22]. It has to be noted that this result is not affected by the initial choice of using the S-wave angular distribution efficiency.

4. With the present statistics it is not possible to discriminate between the two considered annihilation models. Nevertheless the indication of a non negligible D-wave contribution in $\bar{n}p$ annihilation in the interval between 250 and 400 MeV/c was obtained. The value for α_D turns out to be consistent with a more precise determination obtained studying the $\bar{n}p$ annihilation cross section [19].

4. Conclusions

The first measurement of annihilation frequencies of $\bar{n}p$ annihilation into $\pi^+\pi^0$, $\pi^+\eta$ and K^+K_S was performed as a function of the $\bar{n}$ momentum in the range between 50 and 400 MeV/c. These measurements are the first steps to fill the lack of data on specific annihilation channels in the $\bar{n}p$ system at low energy.

The $\pi^+\pi^0$ and K^+K_S elementary branching ratios from $^{33}S_1$ initial state were measured. Hints for the suppression of $K^+\bar{K}^0$ channel from P-wave were obtained while comparable $K\bar{K}$ production rates from $I=0$ and $I=1$ S-wave initial states are observed. The first determination of the contribution of D wave to annihilation in the momentum range up to 400 MeV/c was also obtained and it is in agreement with the one from the fit of the total $\bar{n}p$ annihilation cross section [19].

References

[1] C.B. Dover, T. Gutsche, M. Maruyama, A. Faessler, Prog. Part. Nucl. Phys. 29 (1992) 87.
[2] W. Brückner et al., Z. Phys. A 335 (1990) 217.
[3] OBELIX Coll., A. Adamo et al., Sov. J. Nucl. Phys. 55 (1992) 1732.
[4] F. Iazzi, Proceedings of the First Workshop on Intense Hadron Facilities and Antiproton Physics, Vol. 26, T. Bressani, F. Iazzi, G. Pauli, Eds., (SIF, Bologna, 1990) p. 171.
[5] OBELIX Coll., A. Adamo et al., Phys. Lett. B 287 (1992) 368.
[6] OBELIX Coll., A. Adamo et al., Nucl. Phys. A 558 (1993) 137c.
[7] OBELIX Coll., M. Agnello et al., Phys. Lett. B 337 (1994) 226.
[8] R. Brun et al., GEANT3: Internal Report CERN-DD/EE/84-1, CERN (1987).
[9] A. Bettini et al., Il Nuovo Cimento A 47 (1967) 642.
[10] T. Kalogeropulos, G. Tzanakos, Phys. Rev. D 22 (1980) 2585.
[11] F. Balestra et al., Nucl. Phys A 465 (1987) 714.
[12] A. Bettini et al., Il Nuovo Cimento A 62 (1969) 1038.
[13] M. Agnello et al., Nucl. Inst. Meth. A. to be published.
[14] S. Tessaro. Ph.D. Thesis (1995).
[15] T. Armstrong et al., Phys. Rev. D 36 (1987) 659.
[16] C.J. Batty, Nucl. Phys. A 601 (1996) 425.
[17] J. Mahalanabis et al., Nucl. Phys. A 485 (1988) 546.
[18] J. Jaenicke et al., Z. Phys. A 339 (1991) 297.
[19] OBELIX Coll., A. Bertin et al., Proceedings of the LEAP96 Conference, Dinkelsbuhl, Germany (August 27-31, 1996), in press.
[20] OBELIX Coll., V.G. Ableev et al., Nucl. Phys. A 594 (1995) 375.
[21] OBELIX Collaboration, private communication.
[22] A. Zoccoli, Proceedings of the NAN95 Conference, Moscow, Russia (September 11-16, 1995), Phys. of Atomic Nuclei 59 (1996) 1389.